Materials Science & Engineering A 814 (2021) 141233

Contents lists available at ScienceDirect

Materials Science & Engineering A

journal homepage: http://www.elsevier.com/locate/msea

Microstructural processing of steel at ambient surface temperature

James Kidd [a], Zahabul Islam [a], Daudi Waryoba [b], Aman Haque [a,*]

[a] Mechanical Engineering, Penn State University, University Park, PA, 16802, USA
[b] Engineering, Applied Materials, Penn State University, College Place, DuBois, PA, 15801, USA

ARTICLE INFO

Keywords:
Grains and interfaces
Electron microscopy
Iron alloys
Micromechanics

ABSTRACT

We provide evidence that microstructural processing of metallic materials can be achieved at lower temperatures by passing dc current and simultaneously cooling the specimens. As the Joule heat is removed, the electron wind force due to transfer of momentum to defects become the predominant stimulant for grain boundary and defect migration. We demonstrate this technique on nominally 50 μm thick additive manufactured 316 stainless steel specimens, electrically biased at around 200 A/mm^2 current density while actively cooled to maintain ambient surface temperature. The microstructural analysis involved electron backscattered diffraction, grain boundary misorientation plots, and grain size analysis. Experimental results indicate that both grain growth and grain refinement are possible, depending upon the controlled temperature and processing time. The results also showed significant changes in misorientation angle distributions for both grain growth and grain refinement with almost all low angle grain boundaries being converted to high angle grain boundaries. These results are encouraging for further development of the electron wind force as a driver for low temperature post processing of metals and alloys.

1. Introduction

While the microstructure of metallic materials strongly influences their properties, it is materials processing that determines the various microstructural parameters, such as grain size, texture and dislocation density. Heat treatment has been used for processing since the early history of metallic applications. Particular details vary with the material types or the need for specific properties, but the fundamental mechanism is heat energy activated promotion of diffusion. At lower temperature, mobility of defects and grain boundaries is low enough to make the processing slow. Recrystallization or annealing, for example, requires very high temperatures, ~1000 °C for 316 stainless steel [1] and for long holding periods such as 60 min per inch of thickness. The entire process is a sensitive function of temperature, time and alloying elements. A critical observation motivating this study is that while defect mobility increases with temperature, high temperature can stagnate defects or even create new defects such as voids. For material systems with interfaces, high temperature can also develop thermal stress due to uneven expansion. In this study, we explore non-thermal stimuli such as mechanical force at either ambient or slightly elevated temperatures. If feasible, such non-thermal processing may be time and energy efficient for metallic materials and provide active control of the microstructure and hence material properties. In particular, we investigate the mechanical force field developed in metallic materials when electrical current passes through it. This is also known as the electron wind force (EWF). It is the momentum of moving electrons that is transferred to defects during collisions inside the material [2,3]. This momentum transfer increases atomic mobility of defects in the material. Beyond a critical value, the EWF can induce appreciable grain growth and defect annihilation in a short period of time [4–6]. However, high current density also induces Joule (resistive) heating due to electron scattering in the lattice. Fig. 1 schematically shows the EWF and Joule heating effects in a polycrystalline metal, where the grains are idealized with hexagonal shape.

Fig. 1 also shows a unique feature of the EWF, i.e., it arises from electron-defect interactions. Here, the defects could be the grain substructures comprising of low angle grain boundaries, dislocations, or grain boundaries. In comparison, Joule heating arises from electron-lattice interaction and impacts both grain interior and boundaries. Thus, EWF is a 'just in location' driving force, specific only to defects for their migration or annihilation. It is particularly effective on surface and interface defects such as the grain boundaries, where the electrons lose momentum when flowing from one grain to another due to the differences in crystal orientation. However, the phenomenon requires

* Corresponding author.
E-mail address: mah37@psu.edu (A. Haque).

https://doi.org/10.1016/j.msea.2021.141233
Received 8 January 2021; Received in revised form 2 March 2021; Accepted 1 April 2021
Available online 5 April 2021

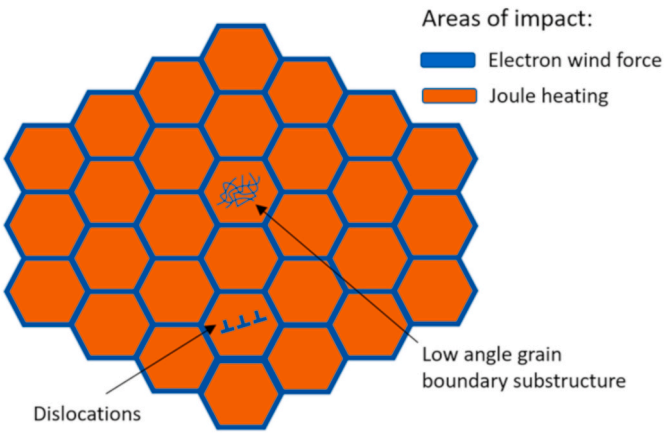

Fig. 1. Schematic showing the areas impacted by Joule heating and electron wind force.

fundamental understanding because it can potentially damage the material through electromigration. Electromigration damage manifests through the EWF but happens at an order of magnitude higher current density in the presence of Joule heat. At lower current densities, the momentum transfer of electrons will promote diffusion, grain boundary migrations, and other microstructural changes. At higher current densities, the momentum transfer will result in mass transport in the material that leads to material damage or failure. Electromigration in copper (Cu) has been studied inside the scanning electron microscopy technique to reveal the void and hillock formation at the cathode and anode ends respectively. The process has an activation energy that depends on the material and microstructure [7]. The magnitude of the force depends on defect types (two dimensional interfaces will scatter the electrons stronger than one dimensional dislocations) and atomic structure [8].

Electrical current effects on microstructural changes have been studied on smaller scales, such as in thin films, to enhance the creation of new phases and grow grain sizes. For example, near-amorphous, 100 nm thick zirconium thin film was shown to re-crystallize under EWF and temperature. The average grain size grew to 150 nm, about 10 times higher than that achieved by thermal annealing alone [9]. Microstructural changes caused by an electrical current have also been achieved on a larger scale using constant and pulsed currents. Constant current has been shown to cause microstructural changes in materials from a couple of recent studies [6,10]. Pulsed current has been much more extensively researched under the term electropulsing. Very high current pulses with width from 20 to 150 micro-seconds have been applied on structural materials, such as aluminum alloys and steel [11–13]. The small pulse width and low frequency result in a negligible rise in temperature. However, this also means extremely fast heating and cooling of the material, similar to a shockwave. Therefore, these studies have reported grain refinement unless the electropulsing is performed at high temperature. The field of powder metallurgy has also explored the use of electrical current to enhance sintering processes [14,15]. These various fields of study have all revealed high-density electric current's ability to improve material properties in ways such as altering grain size, promotion of twin growth, promoting certain phases, or enhancing mobility.

This study focuses on direct constant current, which has been significantly under-researched compared to the general technique of electropulsing, which is characterized by large spikes of increased current density for micro-seconds of duration followed by a lack of current to allow for the material temperature to drop. This temperature drop minimizes the effects of Joule heating while retaining the effects of the EWF. Literature has shown that electropulsing has the ability to alter microstructure in the material but requires very high peak current densities, on the order of 1000 A/mm^2 [16,17]. In this study, we implement specimen cooling under constant direct current to retain the effects of the EWF without the effects of Joule heating. Thus, our steady state technique is different from the electropulsing process.

The electropulsing literature shows evidence of microstructural changes (such as recrystallization, grain refinement, grain growth) that have been debated to be the result of the EWF, Joule heating, or the combination of the two effects. Several studies have suggested that Joule heating plays a role in the dislocation motion and microstructural changes [18–20]. These studies have included alloys such as brass and steel. These materials are not very different from their additive manufactured counterpart; except it is known that the highly non-equilibrium processing conditions increase the defect density in the additive manufactured alloys [21]. The Joule heating explanation for microstructural changes stems from the fact that the generated heat can activate the traditional thermal process. Arguments have also been made that the heat focuses at the grain boundaries which causes the changes in microstructure [18]. The debate is difficult to resolve because the contributions from Joule heating and the EWF are hard to decouple from each other. This explanation does not apply when the microstructural changes occur in samples that were processed at temperatures far below the annealing temperature for a substantially shorter time than what would be used in a thermal annealing process. Meanwhile, the EWF has been suggested to be a definite cause of the microstructural changes by several studies [10,17,22].

To provide convincing evidence towards the benefits of using electricity for post processing of metals, we have designed an experiment that demonstrates EWF for both annealing and refinement of grains in a metal specimen. Additively manufactured 316 stainless steel was chosen for the specimen material, primarily because the high defect density and anisotropy arising from highly non-equilibrium processing conditions. In the next sections, we present the experimental procedures and results for post processing of this material using the EWF in a controlled temperature environment utilizing electron backscatter diffraction (EBSD).

2. Materials & methods

Additively manufactured 316 stainless steel using laser sintering of powder metal was chosen for this study. Powder feedstock with average diameter of 30 μm and purity within ASTM A240 was used with a nitrogen gas atomization process. The sample was printed in a shape of a 1 cm^3 cube then cut into slices of approximately 1 mm thick. These slices were cut parallel to the build direction to reveal the columnar shaped grains. Each slice was grinded down to 150 μm using grit paper. Then the strips were cut into long rectangular shapes of approximately 10 mm long, 0.5 mm wide and 150 μm thick using a dicer machine. From here each strip was individually polished down to approximately 50 μm using various grit paper with the final stage being a grit paper of 1200. The samples were then polished using microfiber pads with diamond, colloidal alumina, and colloidal silica suspensions with particle sizes ranging from 3 μm down to 0.02 μm.

The polished sample was mounted to an aluminum nitride slab that acts as a heat spreader because of its high thermal conductivity and electrical insulation. Copper tape was attached to the aluminum nitride slab to act as electrical contacts on both sides of the sample. The sample was mounted on top of the electrical contacts to make it a free-standing object. Wires were also attached to the copper tape and solder was used on top of the contact pads to enhance the electrical connections. The sample and stage were mounted on a liquid nitrogen temperature-controlled stage inside of an FEI Scios 2 SEM equipped with Focused ion beam (FIB) and energy dipersive spectroscope (EDS) detector. The liquid nitrogen cooled stage allowed for the extraction of heat from the stage to avoid the effects of Joule heating and possible surface contamination in the form of oxidation. The high vacuum conditions and high definition monitoring systems inside the SEM are helpful for in-situ observation of the microstructural changes, particularly at the onset of

subtle changes in the microstructure, and greatly increased the chances of achieving grain growth without failure from the environment. The wires were connected through a feedthrough port in the chamber and connected to a power supply. During the experiment, the current was increased in small increments and held at each current level for a period ranging from about 30 s to a few minutes.

3. Results

EWF-based annealing was performed on the specimens with both passive and active cooling. Passive cooling was achieved by placing the sample on an aluminum nitride slab and then using the massive SEM stage as heat sink. Active cooling was achieved with a temperature control stage with liquid nitrogen flow. We did not observe any discernible changes in microstructure below 150 A/mm^2 current density. However, the annealing process seemed to accelerate thereafter. Irrespective of cooling technique, there is always risk of thermal runaway, a process where thermal stress induced voids localize the temperature leading to failure. We therefore did not exceed the current density limit of 200 A/mm^2, as shown in Fig. 2. Our experience suggests that slightly lower current density than this critical value could be beneficial for the annealing process, although the rate is slower.

As-received Sample: The microstructure of the as-received material as characterized by EBSD is shown in Fig. 3a as an inverse pole figure map in the x-direction (xIPF). The grains appeared to be elongated in one dimension, probably due to the competitive grain growth in additive manufacturing, where grains grow in a direction that is determined by the previously deposited grains and the direction of maximum heat extraction. After performing grain size analysis using the ImageJ software and the line intercept technique, the width of the columnar grains in the as received material was estimated to be around 40 μm. This grain size is typical of a 316 L laser powder bed fusion process [23]. Fig. 3b shows the grain misorientation angle plot obtained from EBSD. A large fraction of the grains had smaller misorientation angles. This suggests high residual stress in the material [24] due to large contractions of the melt pool during solidification.

EWF Annealing with Passive Cooling: While a major objective of this study is to investigate EWF effects at lower temperature, we recognize that the synergy of EWF and moderate levels of temperature can be beneficial for recrystallization and grain growth. To illustrate this, we only passively cooled a fresh specimen at current density around 200 A/mm^2. Fig. 4a shows an EBSD scan of the sample. Interestingly there is a large fraction of annealing twins in the new microstructure. This indicates that EWF applies a high strain rate to the grains during growth that creates the twinning phenomenon. The estimated average grain size from the intercept method is around 75 μm, which is almost double the width of the columnar grains in the as-received material. Plots of the misorientation angles were made for the EBSD scan and can be seen in Fig. 4b. The plot has almost entirely all high angle misorientations. This is the opposite of the as-received scan and

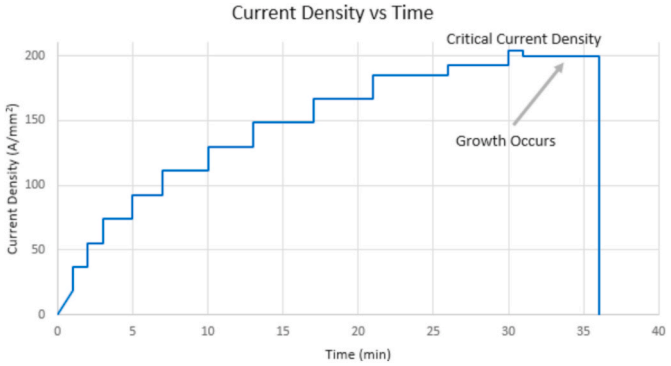

Fig. 2. Current density vs time during a typical EWF annealing experiment.

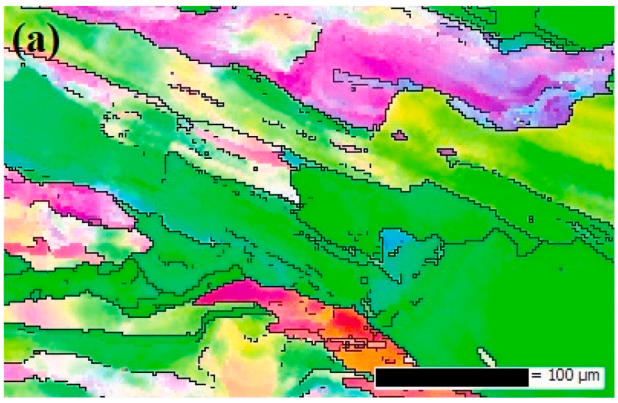

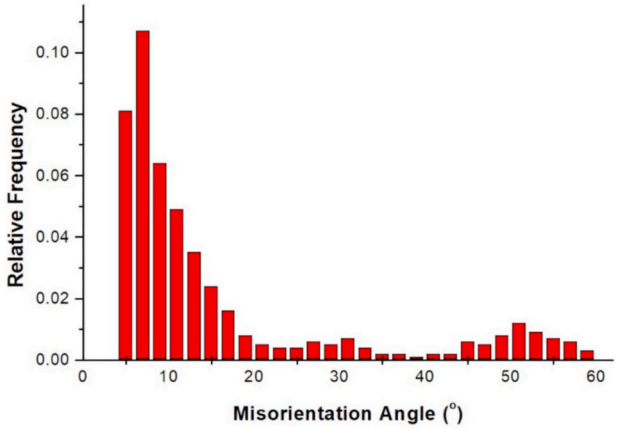

Fig. 3. EBSD of the as-received showing (a) the xIPF map and corresponding (b) misorientation angle plot.

demonstrates how the material is at a lower residual stress level.

EWF Annealing with Active Cooling at Room Temperature: In this processing, we used liquid nitrogen for active cooling of the SEM stage to constrain the specimen surface at room temperature. Fig. 5a shows the EBSD inverse pole figure map to reveal large sized, equiaxed grains and large density of annealing twins. Grain size estimations show the average grain size to be 45 μm. The misorientation angle plot shown in Fig. 5b has almost entirely high misorientation angles. The distribution shows that the microstructure has achieved a lower residual stress state.

We also analyzed residual strain in the as-received and annealed samples with EWF through measurement of local variations/spread in lattice orientations or Kernel Average Misorientation (KAM). KAM displays local orientation changes in the grain and is represented by the average misorientation between every point and its surrounding points, and correlates well with macroscopic plastic strain to highlight regions of high residual strain [25]. The higher the residual strain, the higher the KAM value, and vice versa for low residual strain. It is clear that the as-received specimen (Fig. 6a) exhibited the highest residual strain, distributed throughout the specimen, whereas specimen annealed with EWF and active cooling (Fig. 6c) developed the lowest local strain field with heterogeneous pockets of high strain. Interestingly, specimen annealed with EWF and passive cooling (Fig. 6b) showed intermediate level of residual strain.

Grain Refinement: An interesting observation on the influence of annealing time as a processing parameter is the possibility of grain refinement. In both actively or passively cooled experiments, we clearly

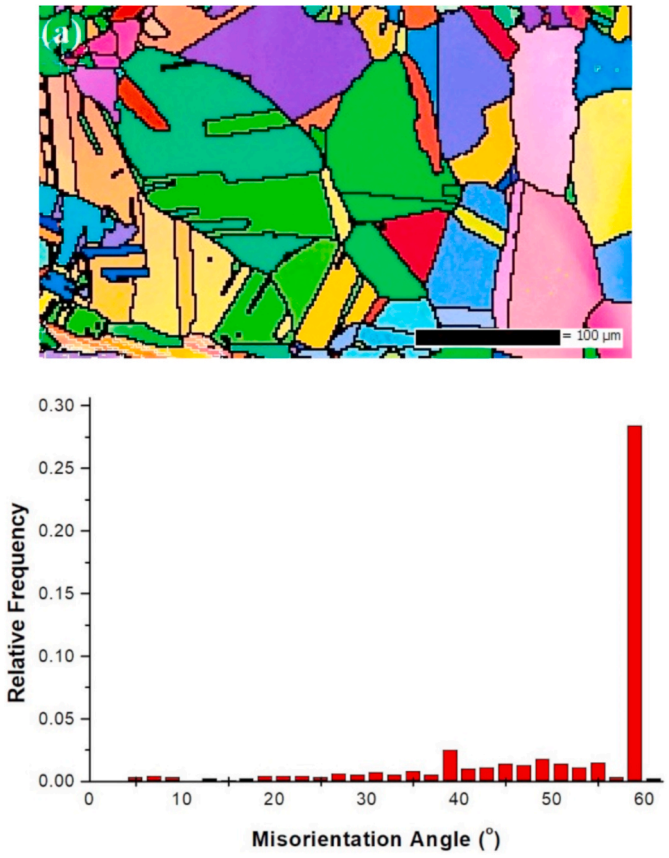

Fig. 4. EBSD of the sample annealed with EWF and passive cooling showing (a) the xIPF map and corresponding (b) misorientation angle plot.

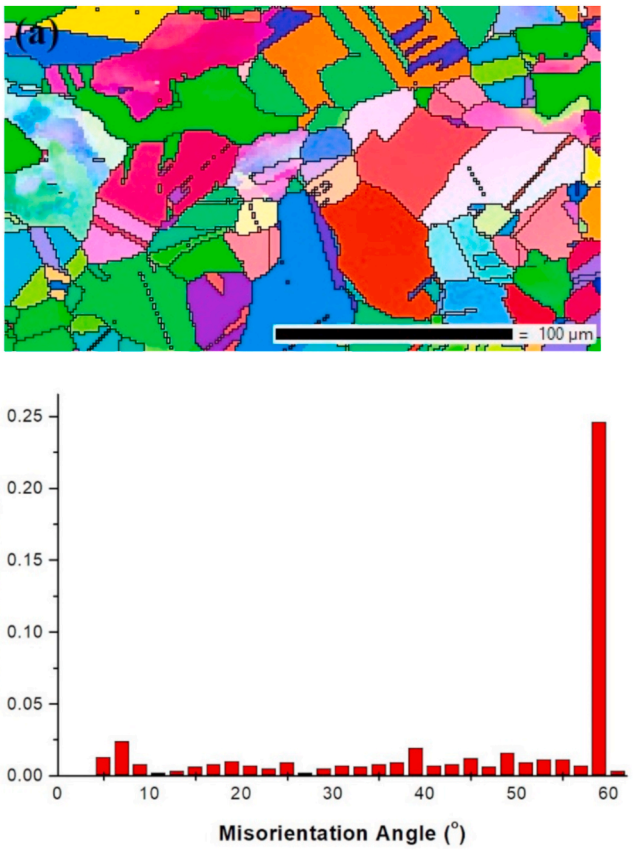

Fig. 5. EBSD of the sample annealed with EWF and active cooling showing (a) the xIPF map and corresponding (b) misorientation angle plot.

observed the transformation of low angle grain boundaries to high angle grain boundaries in a span of about 5 min and at a current density of around 200 A/mm^2. This transformation depends on the dwell time; therefore, the processing time can play important role on the final microstructure. To study this, we did not allow the dwell time (5 min) for a full transformation, rather it was limited to only 2 min. Fig. 7a shows the xIPF map reflecting appreciable amount of grain refinement across the sample. Also, no twinning was observed. Grain size analysis revealed an estimated grain size to be approximately 15 µm. Fig. 7b shows the distribution of misorientation angles in this sample. The comparison of Figs. 3b and 7b shows that, at a dwell time of 2 min, there is a partial transformation of low angle boundaries ($\theta \leq 10°$) to high angle boundaries ($\theta > 10°$). Consequently, the microstructure exhibits a mixture of high and low angle boundaries. The high angles are from the areas of new microstructure and the low angles are from the original microstructure (retained boundaries).

The KAM analysis of this specimen, shown in Fig. 7c, shows a microstructure with residual strain that is lower than the starting microstructure (Fig. 6a) but higher than the specimen annealed with EWF and active cooling (Fig. 6c). However, the residual strain was distributed throughout the specimen as in the starting material. This is indicative of a microstructure undergoing partial transformation.

4. Discussion

In this study, we present experimental evidence of defect removal and microstructural changes at ambient temperature using the EWF. EWF is proposed to be defect-specific, since the force is appreciable only when the electrons are scattered by the defects. In the defect-free lattice, the electrons interact with the lattice atoms only and give rise to Joule heating, but not EWF. Thus, EWF can be viewed as an athermal, just-in-location driving force to mobilize the defects. We suggest that the highly localized nature of this force enables it to disintegrate the immobile defect clusters (for example dislocation sub-structures inside deformed grain that are essentially low angle grain boundaries), even though their global (or average over the specimen cross-section) values are not very high. We also suggest that the EWF is directional (due to the directionality of the electrical current flow), whereas temperature driven defect mobility is mostly random. This could explain why conventional heat treatment requires very long time compared to the EWF-based processing timeframes in this study.

The EBSD scans provide details of microstructural parameters and their evolution. For example, both passively and actively cooled EWF annealed samples transformed to equiaxed grains that coalesced to larger equiaxed grains. However, shorter processing time (even at the same current density) transformed the original microstructure to equiaxed grains but did not allow these grains to complete their grain growth. The new grains formed in these samples can be easily differentiated from the original microstructure since the original grains were elongated in shape. With regards to grain size, passive cooled samples experienced 74% increase in size when comparing columnar grain width to equiaxed grain diameter. Active cooled samples saw a minor grain size increase from 40 µm to about 45 µm. Even with a minor size increament, the microstructure of the room temperature EWF annealed sample still changed drastically since it transformed into equiaxed grain shapes. The grain refinement sample (shorter anneal time) experienced a 74% reduction in grain size when transforming into the small equiaxed grains. The original microstructure also contained more defects inside the grains compared to the newly formed grains. These results are typical of a strain induced grain boundary migration process where the grains bulge from the original shape and have lower dislocation densities.

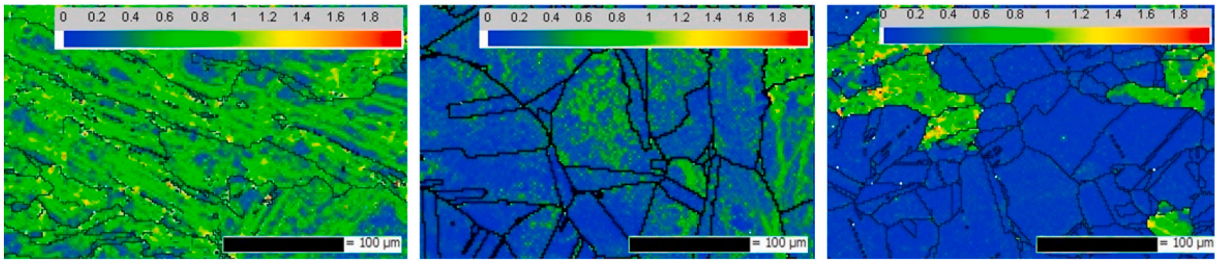

Fig. 6. KAM maps for (a) as-received materials, (b) specimen annealed with EWF and passive cooling, and (c) specimen annealed with EWF and active cooling.

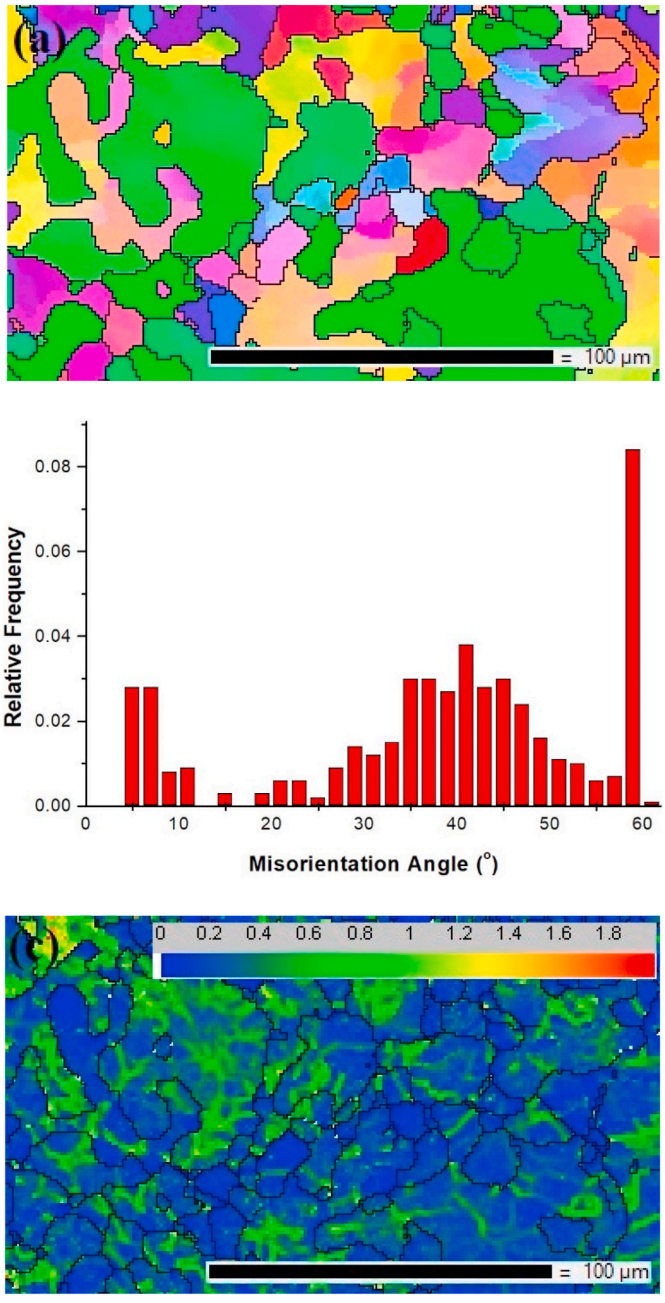

Fig. 7. EBSD of the specimen annealed with EWF and passive cooling for 2 min showing (a) the xIPF map and corresponding (b) misorientation angle plot and (c) KAM map.

The EBSD scans of the passive and actively cooled samples revealed a large number of annealing twins. These twins formed due to the large strain rate that was applied to the grains during the grain growth stage. It is also not surprising that the twins formed in the samples with large grains since large grain sizes have been shown to promote the twinning phenomenon [26,27]. This is also confirmed by the fact that no twins were found in the smaller grains formed in the grain refinement sample shown in Fig. 7a. These twins should be beneficial to the mechanical properties of the samples by increasing the strength and ductility of the samples. The large amounts of twin boundaries should restrict the movement and creation of dislocations. This means that the microstructure can be approximated as an equivalent microstructure of smaller average grain size and therefore larger material strengths [28]. Twins have also been shown to improve ductility of the material beyond what would be seen in a material of similar grain size but without twins [29].

EBSD scans also allowed quantification of the orientation spread as well as the fraction of high and low misorientation angles. For each of the EWF annealed samples, we saw increase in high angle grain boundaries. Studies have shown that scans with large fractions of low angle grain boundaries are evidence that the material is at a high level of stored strain energy [10,30]. Therefore, the resulting plots from our experiments show that the annealing process has reduced the stored strain energy in the sample. This process of analyzing the misorientation angles acts as an easy way to establish optimum processing conditions that ensure complete transformation of the microstructure.

The EBSD scans of the samples that underwent grain refinement showed some unchanged microstructure after processing. It may be that these samples needed more processing time to allow for these grains to be consumed by the bulging new grains. The other possibility is that if the samples were processed further, then the first grains to nucleate would start to grow while other grains are just starting to form. If grains are growing while others are just starting to reform, then the resulting microstructure would have substantial variation in grain size. From the analysis of the grain boundaries (Table 1 and Fig. 8), it can be deduced that at the beginning of EWF annealing, low angle boundaries (LAGBs) are transformed to mostly high angle boundaries (HAGs) with 35°–45°

Table 1
LAGBs, HAGBs, and special boundaries in as-received and annealed specimens.

Specimen	LAGBs (%)	HAGBs (%)		Special Boundaries	
		35°–45° Boundaries	60° Boundaries	Σ3 twins	Σ(9 + 27) twins
As-Received	56.36	3.57	0.31	0.25	0.27
2 min Actively Cooled	13.35	34.30	15.5	18.21	1.50
5 min Actively Cooled	9.49	12.56	48.8	49.52	2.70
5 min Passively Cooled	2.37	14.45	56.6	56.01	3.52

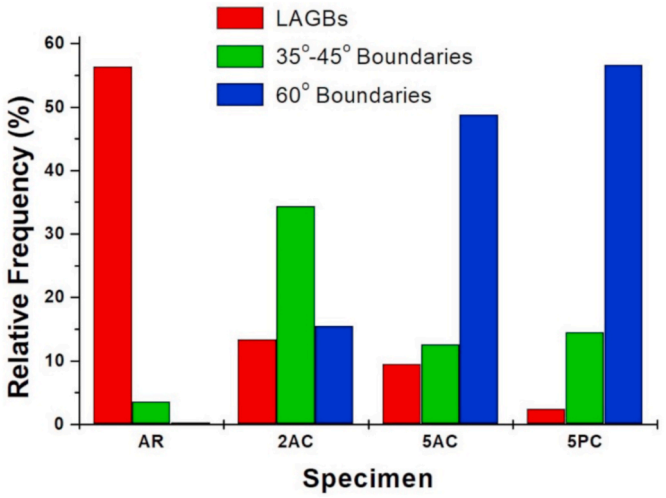

Fig. 8. LAGBs and HAGBs in as-received and annealed specimens (AR – as received; 2AC – 2 min actively cooled; 5AC – 5 min actively cooled; 5 PC - 5 min passively cooled).

boundaries and a few 60° boundaries and latter transformed to mostly 60° boundaries. The 35°–45° boundaries are reported to possess high energy and high mobility, whereas the 60° boundaries, which are mostly Σ3 coherent twin boundaries, have low energy and low mobility (causing a pinning effect) [31]. In general, the ability of the grain boundary to migrate is characterized by the grain-boundary mobility [32], which depends on grain boundary energy, orientation, solute interaction, etc. During grain growth, differences in the grain-boundary mobilities determine the final texture and grain size distribution of a material. In some cases, some grains can grow at the expense of others or may shrink if surrounded by pinning boundaries such as Σ3 coherent twin boundaries [31,33]. It is therefore reasonable to deduce that the 35°–45° HAGBs noted at the intermediate processing time (2 min in this case) are responsible for the grain growth and large grain size that is observed at long processing time (2 min in this case). As they migrate, and coupled with EWF effect, these boundaries are transformed to 60° boundaries (mostly Σ3 twins). Based on the growth accident model [34], the formation of Σ3 boundaries is considered as a result of stacking error at the migrating grain boundaries. The interaction of EWF with mobile boundaries could trigger stacking errors, thereby transforming these boundaries to Σ3 boundaries. It should however be noted that the additional thermal energy for passively cooled specimen could account for the increase in the grain size and the 60° (Σ3) boundaries in this specimen. Annealing twins are usually common in fcc materials with low to medium stacking-fault energy [35].

If the samples need more processing time, then in order to achieve grain refinement the current density should be decreased to allow for more time for the process to take place. This is because, at 200 A/mm^2, the microstructural changes happen very quickly with the original microstructure changing into large grains in a matter of seconds. The samples that underwent grain refinement also saw a large rate of current increase up to the critical current density. This may have influenced the formation of more grain bulging sites (nucleation sites) resulting in a larger number of small grains. If the speed at which the current level is increased to the critical level affects the formation of smaller grains, then the process of refining the grain size would be difficult to control due to the reduced time to detect surface changes. The most reliable way to create a grain refined sample would be to sacrifice on the minimum achievable grain size and allow for a little bit of grain growth to occur to ensure that all the original microstructure has been consumed.

Our experiments indicate that a critical current density is needed to induce rapid (order of minutes) changes in microstructure. For additively manufactured 316 Stainless Steel we found this to be around 200 A/mm^2, which is roughly two orders of magnitude smaller than the electromigration damage level. This is because of the very high initial defect density in the as-received sample. Operating far below the electromigration limit is a beneficial feature. We believe that passive or active cooling further reduces the risk of electromigration damage. The relationship between the current density and time to anneal a material is not a linear relationship. Current densities slightly below the critical value will result in substantially longer processing times. This nonlinear relationship also holds true for larger current densities which means that one can create large microstructural changes in a very short period of time. The differences in processing time at the different current densities may also create different resulting microstructure, but this was not confirmed in this work. The critical current density value is material, composition and mostly, defect density and type dependent.

The samples in this study were processed at a low temperature compared to the temperatures seen in traditional annealing processes. However, exact measurement of internal and surface temperatures is difficult. The actual average temperature in the samples were probably higher than what was measured during the experiment. This is since the temperature was measured on the liquid nitrogen stage, which was a constant 20 °C, not on the sample's surface. Since thermal conductivity of stainless steel (13 W/m-K) is reasonably high and the specimen thickness is very small (about 100 μm), it is expected that the temperature difference is less than 5 °C. It is important to note that any air gap between the specimen and the cooling stage would cause heat to accumulate in the sample and raise the temperature of the material. Our infrared measurements for similar experiments showed relatively low temperatures (on the order of 200 °C), especially when considering that these samples were only passively cooled. These passive cooled temperatures were also confirmed with thermocouple measurements of experiments performed without any cooling stage.

There are ways to estimate how high the temperature was in the cooled samples. For instance, some samples were slightly deformed due to the material trying to expand but were pinned by the electrical connections. This means that temperatures in the sample were large enough for a small size change. This is what first indicated that the sample temperatures were not the same as the cooling stage. A more promising temperature indication of the cooled samples was the fact that the solder had not re-melted during the experiment. This is significant when trying to claim low temperatures because the solder used in this experiment has a very low melting temperature compared to traditional solders. The passively cooled experiments commonly had electrical connection issues due to the solder re-melting, so clearly, the liquid nitrogen cooled stage was working to cool the sample to some value closer to room temperature.

5. Conclusion

In this study, we present passive and active cooling of metallic specimens carrying constant direct current to isolate the electron wind force from Joule heating and use the former to perform low temperature annealing. Processing parameters related to achieving grain bulging and growth in 316 stainless steel were developed with the key parameter being the critical current density of 200 A/mm^2. At this current density, grains grow in short periods of time. This study enhanced the knowledge of how the electron wind force, and not Joule heating, dominates the electric annealing process by creating grain growth at temperatures close to room temperature. This study also provided new information related to how this unique method of strain induced grain boundary migration resulted in a large fraction of annealing twins. These twins formed due to the large strain rates induced by the electron wind force and the large average grain sizes that were obtained. The success of this annealing process was demonstrated by the EBSD data gathered. The large grain sizes and large fraction of annealing twins achieved through this electric annealing process could be clearly identified in the optical images. The EBSD scans confirmed what was seen in the optical images

and showed that the microstructure was at a near equilibrium state since the misorientation angle distributions heavily leaned towards high angles. The short processing times in these experiments seems to be the most beneficial aspect of using this type of grain refinement compared to the long times associated with traditional heat treatments. Even though this process requires large amounts of power, the short period of time at which this power is maintained results in a more energy efficient process compared to traditional heat treatments.

A challenge with this technology is the limitations on size that comes with the large current densities. The maximum size obtained in this study was only in the micron scale due to the available power supplies and cooling solutions. Examples of large amounts of current can be seen in field assisted sintering technology and in electric arc furnaces that have current in excess of 10,000 Amps. With these types of power supplies, parts with cross sectional areas in the centimeters squared size range could be processed in a few minutes. The size scale available for this study limited the feasibility of such analysis. While this study was not able to establish a relationship between the processing parameters and the resultant mechanical properties, there is no doubt that the mechanical properties would be drastically different from the as-received state due to the drastically different microstructures. In terms of energy efficiency, we note that EWF-based annealing not only needs the electrical power as input, but also cooling power to avoid thermal shock or failure. Thus, the input energy can be double of a typical heat treatment process. However, we also note that the time required for the EWF-based process can be 10 times less compared to heat treatment. Therefore, the total energy required can significantly lower compared to conventional heat treatment.

The area of post processing is still dominated by heat treatment. Effect of other stimuli (such as electrical current, as described in this paper) is under-researched and has questions left unanswered. Practical applications of this technology could revolutionize the manufacturing industry and become a standard post processing step due to the energy savings and unique results that have been established by this and other studies. Scaling this technology to meet industrial applications needs to be done. The next logical step in researching this technology would be to increase the sample size. The application of this technology to a standard dog bone shaped sample would require unique power supply and cooling solutions but would undoubtedly result in an excellent process-property relationship and bring this technology one step closer to the industry.

Data availability

The raw/processed data required to reproduce these findings cannot be shared at this time due to technical or time limitations and also the data also forms part of an ongoing study. The authors will make the best efforts to share the raw data upon request.

CRediT authorship contribution statement

James Kidd: Methodology, Investigation, Formal analysis, Writing – original draft. **Zahabul Islam:** Conceptualization, Formal analysis, Validation. **Daudi Waryoba:** Investigation, Formal analysis, Writing – review & editing. **Aman Haque:** Conceptualization, Validation, Writing – review & editing, Funding acquisition.

Declaration of competing interest

The authors declare that they have no known competing financial interests or personal relationships that could have appeared to influence the work reported in this paper.

Acknowledgments

This work was supported by the Division of Civil, Mechanical, & Manufacturing Innovation (Nanomanufacturing program) of the National Science Foundation through award #1760931. The findings and conclusions of this work do not necessarily reflect the view of the National Science Foundation.

References

[1] S. Kheiri, H. Mirzadeh, M. Naghizadeh, Tailoring the microstructure and mechanical properties of AISI 316L austenitic stainless steel via cold rolling and reversion annealing, Mater. Sci. Eng. 759 (2019) 90–96.
[2] Z.-J. Wu, P.S. Ho, Size effect on the electron wind force for electromigration at the top metal-dielectric interface in nanoscale interconnects, Appl. Phys. Lett. 101 (10) (2012) 101601.
[3] K. Crowe, A. Portis, Electron wind-induced muon drift in metals, Hyperfine Interact. 31 (1–4) (1986) 185–189.
[4] H. Conrad, W. Cao, X. Lu, A. Sprecher, Effect of an electric field on the superplasticity of 7475 Al, Scripta Metall. 23 (5) (1989) 697–702.
[5] X. Zhang, H. Li, M. Zhan, Z. Zheng, J. Gao, G. Shao, Electron force-induced dislocations annihilation and regeneration of a superalloy through electrical in-situ transmission electron microscopy observations, J. Mater. Sci. Technol. 36 (2020) 79–83.
[6] D. Waryoba, Z. Islam, B. Wang, A. Haque, Recrystallization mechanisms of Zircaloy-4 alloy annealed by electric current, J. Alloys Compd. 820 (2020) 153409.
[7] Q. Huang, C.M. Lilley, R. Divan, An in situ investigation of electromigration in Cu nanowires, Nanotechnology 20 (7) (2009), 075706.
[8] C. Tao, W. Cullen, E. Williams, Visualizing the electron scattering force in nanostructures, Science 328 (5979) (2010) 736–740.
[9] Z. Islam, B. Wang, A. Haque, Current density effects on the microstructure of zirconium thin films, Scripta Mater. 144 (2018) 18–21.
[10] D. Waryoba, Z. Islam, B. Wang, A. Haque, Low temperature annealing of metals with electrical wind force effects, J. Mater. Sci. Technol. 35 (4) (2019) 465–472.
[11] H. Xiao, Z. Lu, K. Zhang, S. Jiang, C. Shi, Achieving outstanding combination of strength and ductility of the Al-Mg-Li alloy by cold rolling combined with electropulsing assisted treatment, Mater. Des. 186 (2020) 108279.
[12] F. Wang, D. Qian, L. Hua, H. Mao, L. Xie, Voids healing and carbide refinement of cold rolled M50 bearing steel by electropulsing treatment, Sci. Rep. 9 (1) (2019) 1–7.
[13] Y. Sheng, Y. Hua, X. Wang, X. Zhao, L. Chen, H. Zhou, J. Wang, C.C. Berndt, W. Li, Application of high-density electropulsing to improve the performance of metallic materials: mechanisms, microstructure and properties, Materials 11 (2) (2018) 185.
[14] T. Kondo, T. Kuramoto, Y. Kodera, M. Ohyanagi, Z.A. Munir, Influence of pulsed DC current and electric field on growth of carbide ceramics during spark plasma sintering, J. Ceram. Soc. Jpn. 116 (1359) (2008) 1187–1192.
[15] J.E. Garay, Current-activated, pressure-assisted densification of materials, Annu. Rev. Mater. Res. 40 (1) (2010) 445–468.
[16] W. Zhang, M.L. Sui, Y.Z. Zhou, D.X. Li, Evolution of microstructures in materials induced by electropulsing, Micron 34 (3) (2003) 189–198.
[17] Z.N. Yang, F. Jiang, X.B. Wang, L. Qu, Y.G. Li, L.J. Chai, F.C. Zhang, Effect of electropulsing treatment on microstructure and mechanical properties of a deformed ZrTiAlV alloy, Materials 12 (21) (2019) 3560.
[18] M.-J. Kim, K. Lee, K.H. Oh, I.-S. Choi, H.-H. Yu, S.-T. Hong, H.N. Han, Electric current-induced annealing during uniaxial tension of aluminum alloy, Scripta Mater. 75 (2014) 58–61.
[19] R. Fan, J. Magargee, P. Hu, J. Cao, Influence of grain size and grain boundaries on the thermal and mechanical behavior of 70/30 brass under electrically-assisted deformation, Mater. Sci. Eng. 574 (2013) 218–225.
[20] J.J. Jones, L. Mears, Thermal response modeling of sheet metals in uniaxial tension during electrically-assisted forming, J. Manuf. Sci. Eng. 135 (2) (2013).
[21] L. Yuan, Solidification defects in additive manufactured materials, JOM 71 (9) (2019) 3221–3222.
[22] K. Han, S. Qin, H. Li, J. Liu, Y. Wang, C. Zhang, P. Zhang, S. Zhang, H. Zhang, H. Zhou, EBSD study of the effect of electropulsing treatment on the microstructure evolution in a typical cold-deformed Ni-based superalloy, Mater. Char. 158 (2019) 109936.
[23] P.Z. Chenfan Yu, Zhefeng Zhang, Wei Liu, Microstructure and fatigue behavior of laser-powder bed fusion austenitic stainless steel, J. Mater. Sci. Technol. 46 (2020) 191–200, 0.
[24] P. Molnár, A. Jäger, P. Lejček, The role of low-angle grain boundaries in multi-temperature equal channel angular pressing of Mg–3Al–1Zn alloy, J. Mater. Sci. 47 (7) (2012) 3265–3271.
[25] M. Kamaya, A.J. Wilkinson, J.M. Titchmarsh, Quantification of plastic strain of stainless steel and nickel alloy by electron backscatter diffraction, Acta Mater. 54 (2) (2006) 539–548.
[26] J.W. Christian, S. Mahajan, Deformation twinning, Prog. Mater. Sci. 39 (1) (1995) 1–157.
[27] R.A. Varin, J. Kruszynska, Control of annealing twins in type 316 austenitic stainless steel, Acta Metall. 35 (7) (1987) 1767–1774.
[28] C.S. Pande, B.B. Rath, M.A. Imam, Effect of annealing twins on Hall–Petch relation in polycrystalline materials, Mater. Sci. Eng. 367 (1) (2004) 171–175.
[29] D.R. Steinmetz, T. Jäpel, B. Wietbrock, P. Eisenlohr, I. Gutierrez-Urrutia, A. Saeed–Akbari, T. Hickel, F. Roters, D. Raabe, Revealing the strain-hardening behavior of twinning-induced plasticity steels: theory, simulations, experiments, Acta Mater. 61 (2) (2013) 494–510.

[30] G.M. Karthik, S. Panikar, G.D.J. Ram, R.S. Kottada, Additive manufacturing of an aluminum matrix composite reinforced with nanocrystalline high-entropy alloy particles, Mater. Sci. Eng. 679 (2017) 193–203.
[31] O. Engler, On the influence of orientation pinning on growth selection of recrystallisation, Acta Mater. 46 (5) (1998) 1555–1568.
[32] C.C. Yang, A.D. Rollett, W.W. Mullins, Measuring relative grain boundary energies and mobilities in an aluminum foil from triple junction geometry, Scripta Mater. 44 (12) (2001) 2735–2740.
[33] D.R. Waryoba, P.N. Kalu, R. Crooks, Grain-boundary structure of oxygen-free high-conductivity (OFHC) copper subjected to severe plastic deformation and annealing, Mater. Sci. Eng. 494 (1) (2008) 47–51.
[34] C.M. Barr, A.C. Leff, R.W. Demott, R.D. Doherty, M.L. Taheri, Unraveling the origin of twin related domains and grain boundary evolution during grain boundary engineering, Acta Mater. 144 (2018) 281–291.
[35] O. Mishin, G. Gottstein, Grain boundary ensembles due to grain growth in copper with strong recrystallization texture, Mater. Sci. Eng. 249 (1–2) (1998) 71–78.